PHYTOGEOGRAPHY ASSOCIATED AT SPECTRAL ABSORPTION SHAPES IN THE SOUTHERN REGION OF THE CALIFORNIA CURRENT

EDUARDO MILLÁN-NÚÑEZ
Centro de Investigación Científica y de Educación Superior de Ensenada
Departamento de Ecología Marina
Carretera Ensenada-Tijuana No. 3918
Fraccionamiento Zona Playitas, C.P. 22860
Ensenada Baja California, México
ph: + 52 (646) 1750500, fax: +52 (646) 1750574
emillan@cicese.mx

MARIANA MACÍAS-CARBALLO
Universidad Autónoma de Baja California
Facultad de Ciencias Marinas
Km 103 Carretera Tijuana-Ensenada, Apartado Postal #453
Ensenada, B.C., C.P. 22880, México
mariana_macias33@hotmail.com

ABSTRACT

The phytogeographic association of nano-microphytoplankton was characterized during April 2008 in the southern region of the California Current with 21 diatom and 11 dinoflagellate genera. Hierarchization of the diatom community (>5 μm) revealed 12 persistent genera throughout the study area. Two bloom events were detected: one in San Quintín Bay dominated by *Eucampia zodiacus* (646×10^3 cells L^{-1}) and another of lesser intensity off Punta Eugenia dominated by *Pseudo-nitzschia* spp. Both blooms were attributed to upwelling events in the region when the $25\sigma_\theta$ surface was inclined from between 80 and 30 m. The intrusion of two water masses was observed: high-nutrient low-chlorophyll Subarctic Water, influencing the stations off Ensenada and San Quintín Bay; and California Current water, influencing the stations off Punta Eugenia. The magnitude of the specific absorption coefficient of phytoplankton (a^*_{ph}) showed large variability in the blue Soret band (440 nm), while the blue/red ratio of absorption ($a_{ph}440/a_{ph}674$) ranged from 1.7 to 7.4, both with high values at offshore stations. Our $a^*_{ph}440$ and b/r ratio results indicated an inverse behavior in the community size distribution. The diatom community (>5 μm) showed four phytogeographic provinces with six different pattern curves from normalized spectral absorption shapes ($a_{ph}n/440$ nm). We concluded that the southern region of the California Current consists of a basic structure composed of smaller cells and few microphytoplankton cells that maintains a balanced community periodically, an extra diatom population is superimposed on the basic structure, resulting in high values of the absorption coefficient of phytoplankton and a better hierarchical phytoplankton structure in the upwelling system.

INTRODUCTION

Phytoplankton community size structure and primary production are the two main factors defining the importance of a pelagic ecosystem. This information provides knowledge of the biogeographic association and the coupling between biological and environmental factors at different scales. Recently, marine scientists have indicated the need for improved techniques to detect the variability in plankton ecology at small and interannual time series, since changes in the community structure of organisms are controlled primarily by local or regional processes. Pelagic ecosystem response to interannual variability off Baja California has been previously described (Gaxiola-Castro et al. 2008), and an acceptable compatibility was found using climate indices such as the Pacific Decadal Oscillation (PDO; Mantua et al. 1997), and Multivariate ENSO Index (MEI; Wolter and Timlin 1998). During the period 2002–06, under weak El Niño conditions, a decrease in plankton organisms of the pelagic system was observed in the southern region of the California Current (Venrick et al. 2003; Durazo 2009; Millán-Núñez and Millán-Núñez 2010); whereas an increase in organisms was observed in 2001 and 2008, under La Niña conditions (Millán-Núñez et al. 2004; Baumgartner et al. 2008). This study thus aims to contribute to the knowledge of the phytoplankton geography association in the southern region of the California Current under La Niña conditions.

METHODS

The Mexican California Current research program (IMECOCAL, acronym for Investigaciones Mexicanas de la Corriente de California) monitors 91 stations distributed from northern transect 100 off Ensenada to southern transect 137 to the south of Punta Abreojos; however, only 45 stations were surveyed during the cruise conducted from 16 to 30 April 2008 due to the prevailing weather (fig. 1). Temperature and salinity were measured to 1000 m depth (depending on the topography) using a SeaBird SBE-911 CTD fitted with a rosette holding 5-L Niskin bottles. The biological samples were taken at 10 m depth. Phytoplankton samples were stored in 250 mL dark bottles, preserved in 4% formaldehyde, and neutralized with sodium borate at pH between 7.5 and 8 (Throndsen 1978). To obtain the light absorption coefficients of phytoplankton (a_{ph}), one litre of seawater was filtered through Whatman glass fiber filters (GF/F, 25 mm), which were stored in HistoPrep® capsules and deposited in a liquid nitrogen container for subsequent analysis in the laboratory.

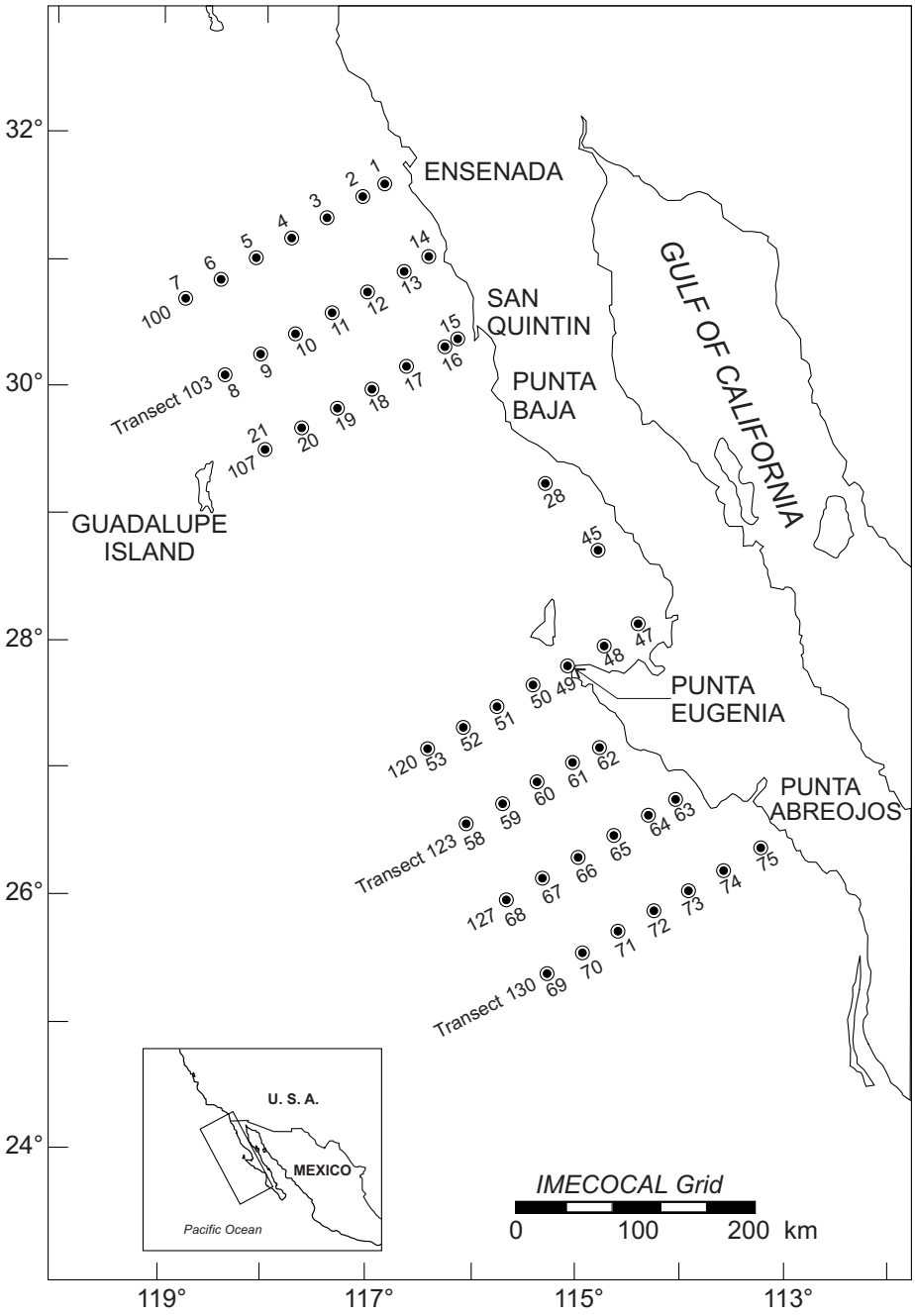

Figure 1. Study area and location of the stations sampled during April 2008 off Baja California. Samples were taken at 10 m depth.

Nano-microphytoplankton (>5 μm). The analysis of nano-microphytoplankton was carried out within the first two months after the cruise, using an inverted microscope at 160× and 400× magnification (Utermöhl 1958) with a sedimentation chamber of 50 mL. The qualitative and quantitative classifications of nano-microdatoms were made to the genus level and whenever possible to the species level (Moreno et al. 1997; Tomas 1997). The genera were sorted according to the Niche Amplitude Index (Levins 1978), where the level position of the taxa represent the major spatial distribution between the sampling stations. The association between nano-microdiatoms was then determined using dendrograms based on the unweighted pair group method with arithmetic mean (UPGMA; Sokal and Rohlf 1962) in relation to the first 12 genera present in the Table 1a and Table 1b.

Absorption coefficient of phytoplankton (a_{ph}). The GF/F filters were analyzed in the first two weeks after the cruise. The reference and sample filters were kept sat-

TABLE 1A

Spatial distribution of the Niche Amplitude Index from nano-microphytoplankton genus at 10 m depth during April 2008. The lowest fraction number represents the dominant cells. Station 1–47.

Stations	1	2	3	4	6	7	9	10	11	12	13	14	15	16	17	18	19	28	45	47
Diatoms																				
1. *Nitzschia*	0.091		0.018	0.007		0.008	0.010	0.025				0.013		0.053	0.020				0.009	0.069
2. *Coscinodiscus*			0.051	0.019	0.102		0.028			0.038	0.076	0.004		0.005	0.083	0.131			0.003	0.024
3. *Naviculа*			0.071			0.162								0.034		0.041		0.002		
4. *Chaetoceros*												0.302	0.059			0.060			0.103	0.007
5. *Thalassionema*	0.037			0.039									0.005	0.075	0.225			0.003	0.028	0.079
6. *Pseudo-nitzschia*						0.036												0.001		
7. *Rhizosolenia*														0.012	0.000					0.014
8. *Eucampia*													0.339	0.017				0.469	0.130	
9. *Thalassiosira*													0.157					0.023	0.761	
10. *Actinoptychus*																				
11. *Guinardia*												0.023								
12. *Pseudoeunotia*																				1.000
Hemiaulus																				0.129
Ditylum												0.098	0.364					0.122	0.105	0.061
Leptocylindrus																			0.264	
Asterionella																				
Gramatophora																				
Corethron																				
Planktoniella																			1.000	
Skeletonema													1.000							
Dinoflagellates																				
Gymnodinium	0.009	0.161	0.027	0.010	0.054	0.012	0.029	0.036	0.080	0.020	0.080	0.007	0.002	0.014					0.003	0.003
Ceratium			0.039	0.205			0.085	0.052	0.078	0.058		0.015	0.007	0.024		0.067		0.002	0.001	
Gyrodinium				0.044	0.235		0.064	0.078		0.088		0.005	0.002		0.064			0.005	0.003	
Prorocentrum	0.059											0.007	0.004	0.035						
Scrippsiella								0.223				0.013			0.182			0.005		0.008
Protoperidinium			0.161				0.351	0.214		0.241			0.005					0.003		0.008
Gonyaulax			0.062	0.046			0.135	0.083	0.124	0.093	0.186	0.010		0.013				0.001		
Dinophysis				0.215						0.431			0.002							
Oxytoxum				0.109		0.249			0.291									0.002		
Peridinium													0.008			0.918		0.009		
Pyrocystis													0.058	0.779						

TABLE 1B

Spatial distribution of the Niche Amplitude Index from nano-microphytoplankton genus at 10 m depth during April 2008. The lowest fraction number represents the dominant cells. Station 48–75.

Stations	48	50	51	52	53	58	59	60	61	62	63	64	65	66	67	68	69	70	71	72	73	74	75	
Diatoms																								**Bi(%)**
1. *Nitzschia*	0.017	0.002	0.001	0.048	0.004	0.022		0.009	0.064	0.065	0.061	0.051	0.042	0.018		0.047	0.037		0.032		0.041	0.083	0.031	73.294
2. *Coscinodiscus*	0.005	0.001	0.001	0.019	0.001	0.061				0.005	0.028	0.116						0.153					0.046	2.006
3. *Navicula*		0.002	0.002	0.018	0.009		0.113			0.002	0.004	0.283	0.087			0.119			0.041				0.009	0.723
4. *Chaetoceros*		0.026	0.005		0.014		0.197				0.013	0.046		0.105									0.063	0.330
5. *Thalassionema*	0.003	0.006	0.002	0.039						0.014	0.039	0.269			0.124								0.014	0.292
6. *Pseudo-nitzschia*	0.036	0.165	0.236	0.016	0.212			0.104		0.077	0.050	0.047				0.013							0.007	0.312
7. *Rhizosolenia*	0.460	0.012	0.004	0.044	0.030			0.058		0.011	0.009	0.094		0.233		0.018								0.123
8. *Eucampia*		0.044																						0.057
9. *Thalassiosira*		0.059																						0.041
10. *Actinoptychus*																					0.599	0.401		0.034
11. *Guinardia*											0.035												0.941	0.032
12. *Pseudoeunotia*																								0.026
Hemiaulus		0.177	0.090								0.035	0.570												0.027
Ditylum		0.250																						0.028
Leptocylindrus			0.078							0.082		0.576												0.024
Asterionella		1.000																						0.025
Gramatophora					1.000																			0.021
Corethron											1.000													0.021
Planktoniella																								0.021
Skeletonema																								0.024
Dinoflagellates																								
Gymnodinium	0.001	0.001		0.010				0.054	0.027	0.001	0.002	0.022	0.025	0.040	0.032	0.004		0.080	0.092		0.040	0.013	0.008	20.553
Ceratium	0.005	0.003	0.001			0.094	0.063					0.025			0.094	0.025					0.058			0.948
Gyrodinium		0.002		0.088	0.002	0.141			0.059	0.008	0.002	0.038	0.054										0.016	0.356
Prorocentrum	0.005			0.063		0.201		0.084			0.003		0.078				0.335				0.126			0.142
Scrippsiella		0.005							0.334	0.008		0.054										0.167		0.064
Protoperidinium			0.002							0.015														0.064
Gonyaulax																	0.248							0.219
Dinophysis										0.007					0.345									0.055
Oxytoxum															0.348									0.062
Peridinium		0.015								0.049														0.030
Pyrocystis		0.108	0.055																					0.023

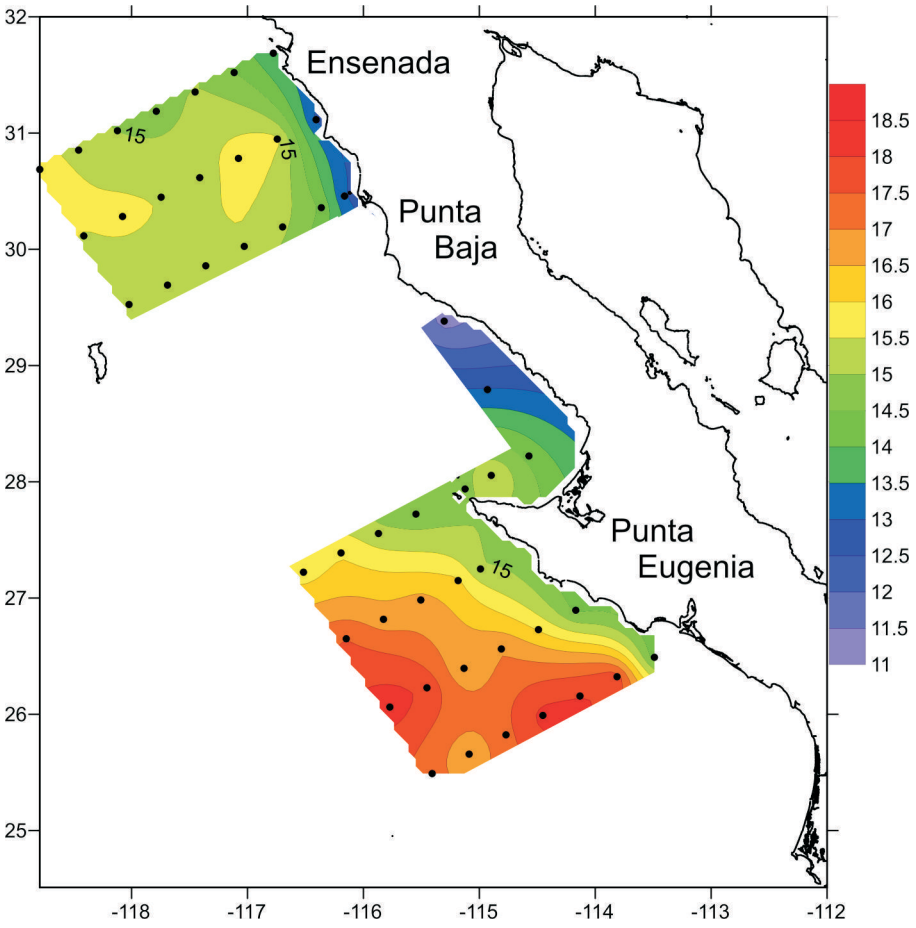

Figure 2. Spatial distribution of temperature (°C) at 10 m depth during April 2008.

urated during the analysis with filtered seawater (0.2 μm) and measured in a Shimadzu UV-2401 PC spectrophotometer equipped with an integrating sphere (Cleveland and Wiedemann 1993). The samples were measured between 400 and 750 nm with 1 nm sampling interval, 2 nm slit width, and medium speed of 330 nm min^{-1}; the filters were then rinsed in methanol for 15 minutes (Kishino et al. 1985). The spectral curves of the absorption coefficient were corrected by two factors: baseline correction (reference filter) and path-length amplification (β) by adjusting the optical density of the filtered samples (OD_{fil} (λ)) to the optical density of samples in suspension (OD_{sus} (λ)) (Mitchell 1990) (equation 1). The a_{ph} was taken to be the difference between the absorption coefficient of total particulate matter (a_p) and the absorption coefficient of detritus (a_{det}), and the specific absorption coefficient of phytoplankton (a^*_{ph}, m^2 (mg Chl *a*)$^{-1}$) was obtained by normalizing the phytoplankton absorption data (m^{-1}) by the concentration of chlorophyll *a* (Chl *a*, mg m^{-3}) extracted with 90% acetone by fluorometric analysis. The phytoplankton spectral shape ($a_{ph}n$) was obtained by analyzing a_{ph} (m^{-1}) normalized by the area below the curve between 400 and 750 nm (equation 2). To determine the homogeneity of slopes between 440–550 nm we used a linear model fitted by least squares (Macías-Carballo 2011).

$$OD_{sus} = 0.3385\ OD_{filt} + 0.4770\ (OD_{filt})^2 \quad (1)$$

$$a_{ph}n = \frac{a_{ph}(\lambda)(m^{-1})}{\int_{400}^{750} a_{ph}(\lambda)(m-1)\delta\lambda(nm)} \quad (2)$$

RESULTS

Oceanographic characterization. Authors such as McClatchie et al. 2009 have reported oceanographic conditions in the California Current System along the West Coast of North America in 2008 and 2009. During this period, the principal oceanographic forcing on the California Current was determined to be a La Niña event, its main characteristics prevailing since mid-2007 to early 2009. A cold phase was detected in relation to El Niño-Southern Oscillation (ENSO), as was also observed during 1998–99 (Bjorkstedt et al. 2010). A new phase of El Niño-La Niña conditions occurred in the

TABLE 2

Trans = transects showing a subset of the original CalCOFI grid, sta = stations, temp (T °C), salinity, diatoms (cells L^{-1}), dinoflag (cells L^{-1}), specific absorption coefficient of phytoplankton (a^*_{ph}, m^2 (mg Chl *a*)$^{-1}$) at 440 nm, blue/red ratio ($a_{ph}440/a_{ph}674$ nm), chlorophyll *a* (mg m^{-3}) from 10 m samples collected during April 2008.

Trans	Sta	Temp	Salinity	Diatoms	Dinoflag	$a^*_{ph}440$	Ratio	Chl *a*
100.30	1	13.59	33.732	2063	552	0.053	2.35	4.89
100.35	2	15.07	33.596	0	0	0.038	2.76	1.19
100.40	3	15.06	33.452	966	690			
100.45	4	14.68	33.301	414	1794		2.96	0.42
100.50	5	14.99	33.247					
100.55	6	15.35	33.361	138	276	0.050	3.04	0.17
100.60	7	15.73	33.444	1514	414	0.024	7.40	0.15
103.60	8	15.48	33.304			0.050	2.74	0.17
103.55	9	15.62	33.361	276	1242			0.18
103.50	10	15.48	33.332	276	966	0.048	3.64	0.21
103.45	11	15.30	33.345	0	826			0.23
103.40	12	15.68	33.461	141	828			0.25
103.35	13	15.63	33.588	138	414			0.52
103.30	14	12.91	33.885	18565	2342	0.002	1.61	5.46
107.32	15	13.05	33.883	1021677	42624	0.023	1.79	15.2
107.35	16	14.41	33.749	6326	1654			4.32
107.40	17	15.10	33.552	1240	276	0.027	3.03	0.72
107.45	18	15.47	33.525	414	414	0.037	2.74	0.45
107.50	19	15.10	33.340	688	276	0.038	3.82	0.34
107.55	20	15.10	33.346					
107.60	21	15.10	33.343					
113.30	28	11.32	33.753	197735	3850	0.015	1.83	7.43
117.30	45		33.765	111448	4125	0.009		11.2
120.30	47	14.33	33.714	108627	10999	0.042	1.89	11.4
120.35	48	15.56	33.678	27026	690	0.040	1.88	0.18
120.40	49	14.78	33.690					7.87
120.45	50	14.67	33.733	129972	3270	0.030	1.69	0.12
120.50	51	15.40	33.718	223312	1100	0.032	1.72	3.78
120.55	52	15.96	33.689	1652	552	0.042	2.47	1.24
120.60	53	15.71	33.690	53489	138	0.031	2.47	2.01
123.60	58	17.49	33.730	276	552			0.23
123.55	59	16.71	33.525	1787	276	0.049	4.94	0.17
123.50	60	16.65	33.542	963	688			0.30
123.45	61	16.09	33.720	962	1100	0.036	2.79	1.13
123.40	62	15.05	33.818	68572	2750	0.029	1.94	7.05
127.35	63	14.38	33.683	67143	1145	0.036	2.14	6.03
127.40	64	15.96	33.661	14025	1377	0.038	2.29	1.00
127.45	65	16.97	33.674	1237	552	0.046	4.06	0.44
127.50	66	16.52	33.605	1238	412	0.037	3.76	0.38
127.55	67	17.92	33.750	138	552			0.15
127.60	68	18.22	33.778	3700	316	0.027	6.33	0.14
130.60	69	14.23	33.553	138	276	0.016	5.57	0.23
130.55	70	16.65	33.706	138	138	0.052	5.82	0.19
130.50	71	17.34	33.645	414	0			0.31
130.45	72	18.15	33.744	552	690	0.033	5.55	0.30
130.40	73	17.99	33.721	552	552	0.053	5.73	0.28
130.35	74	17.81	33.689	1375	276	0.030	2.79	0.31
130.30	75	14.23	33.883	23098	1784	0.022	2.17	9.49

southern region of the California Current during late 2006–07 and 2007–08, respectively, depicted by a transition from moderately positive temperature and salinity anomalies during winter 2006–07, to slightly cool and fresh conditions giving place to La Niña conditions that continued until spring 2008. Likewise, results from biological indicators suggest an increase in the abundances of life cycles and composition of phytoplankton communities (Durazo 2009; Millán-Núñez 2010).

In this study, water temperatures at 10 m depth ranged from 11.32°C to 18.22°C and were distinguished as: temperate waters of ~15.2°C off Punta Eugenia and northern Baja California, cold waters of ~11.5°C (this indicates active upwelling) to the south of San Quintín and Punta Baja; and warm waters of ~17.5°C in the oceanic area off Punta Eugenia (fig. 2). Salinity at 10 m depth ranged from 33.25 to 33.90, with low salinity water detected at stations off the coast of northern Baja California (table 2). In this cruise, three water masses have been documented off Baja California (García-

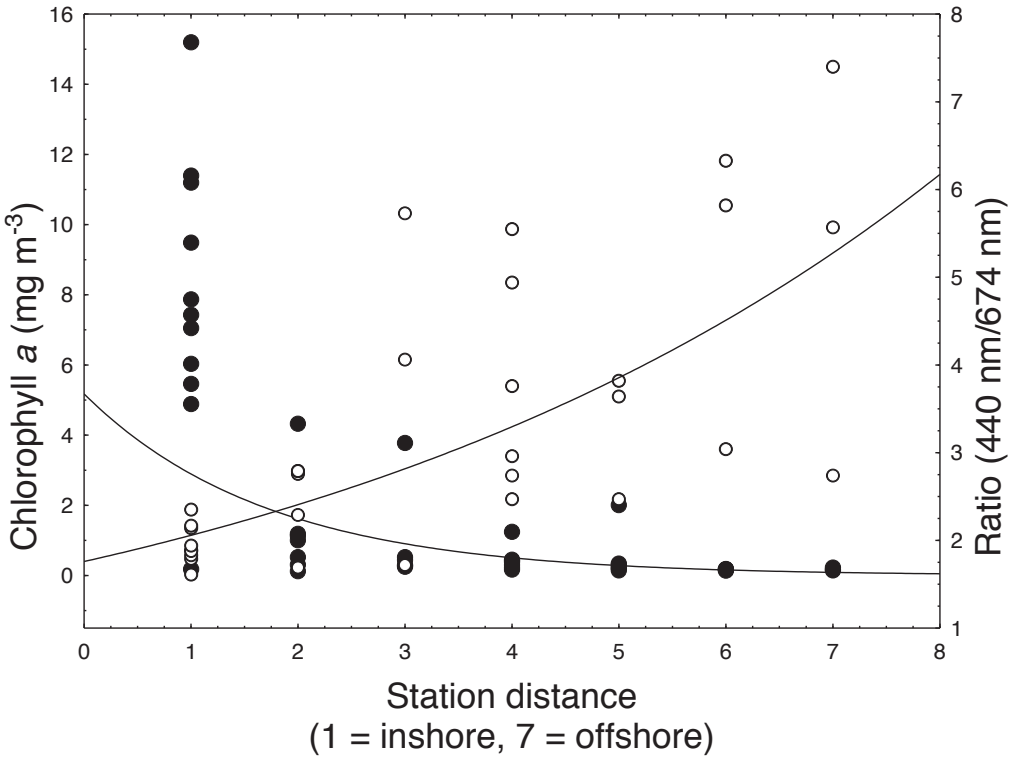

Figure 3. The absorption coefficient phytoplankton ratio at two wavelength (440 nm/674 nm) (clear circles), and chlorophyll *a* concentration (dark circles). The stations are numbered as: #1 nearshore station; #7 offshore station.

Córdova, 2008), except at 10 m depth, where only two were detected: Subarctic Water (SAW) and California Current Water (CCW).

Nano-microphytoplankton (>5 μm). The spatial distribution of nano-microphytoplankton in San Quintín Bay showed a maximum of 1064×10^3 cells L^{-1} (sta. 15), while the mean values of diatoms and dinoflagellates were ~154×10^3 cells L^{-1} and ~4.6×10^3 cells L^{-1}, respectively (table 2). The taxonomic composition of phytoplankton comprised 21 diatoms genera, 11 dinoflagellates, and 2 silicoflagellates (scant presence of *Dictyocha* sp. and *Distephanus* sp.) (table 1a and 1b). The most abundant diatom genera throughout the study area were *Nitzschia* sp., *Coscinodiscus* sp., *Navicula* sp., *Chaetoceros* sp., *Thalassionema* sp., *Pseudo-nitzschia* sp., *Rhizosolenia* sp., *Eucampia* sp., *Thalassiosira* sp., *Actinoptychus* sp., *Guinardia* sp., and *Fragilariopsis* sp. The dominant dinoflagellate genera were *Gymnodinium* sp., *Ceratium* sp., *Gyrodinium* sp., and *Prorocentrum* sp. The genus *Nitzschia* spp. was the most persistent, showing five species: *N. closterium* Ehrenberg (or *Cylindrotheca closterium*), *N. seriata* Cleve, *N. sigmoidea*, and two unidentified species. The abundance of the genera *Nitzschia* spp. and *Pseudo-nitzschia* sp. were observed with high values of ~210×10^3 cells L^{-1} in the area off Punta Eugenia, as was the abundance of *Eucampia zodiacus* Ehrenberg and *Eucampia cornuta* (Cleve) Grunow, showing values of ~646×10^3 cells L^{-1} and ~80×10^3 cells L^{-1}, respectively, to the north of Punta Baja (table 2).

Specific absorption coefficient of phytoplankton (a^*_{ph}). Values of a^*_{ph} 440 nm ranged from 0.002 to 0.053 m^2 (mg Chl *a*)$^{-1}$ (table 2). The spectral curves with lower a*ph 440 nm were located at inshore stations to the north of San Quintín and south of Punta Baja, respectively. In station 47 the absorption coefficient of phytoplankton ($a_{ph}440$) ranged from 0.003 and 0.489 (m^{-1}), and at 674 nm it showed a maximum of 0.258 (m^{-1}) ($a_{ph}674$ data not shown). The B/R ratios ($a_{ph}440/a_{ph}674$) ranged from 1.6 to 7.4, with high values at offshore stations (fig. 3).

Phytoplankton associations and spectral absorption shapes. This study shows four clusters when the stations were associated on the abundance of the 12 main genera of nano-microdiatoms (fig. 4). After the cluster it is transformed as a map or phytogeographic provinces (PGPv) (fig. 5). The first PGPv (A) was dominated by *Eucampia* spp., while PGPv (B) was dominated by *Pseudo-nitzschia* spp. The third PGPv (C_{North}, C_{South}) was formed by a mixture of species of diverse genera (*Thalassiosira* sp., *Chaetoceros* spp., *Nitzschia* spp.), as was the fourth PGPv (D_{North}, D_{South}) (*Thalassionema* sp., *Coscinodiscus* spp., *Guinardia* sp., *Actinoptychus* sp., *Rhizosolenia* spp., *Fragilariopsis* sp., *Navicula* spp.). Figure 6 shows six pattern curves (M1–M6) associated at 32 spectral absorption shapes

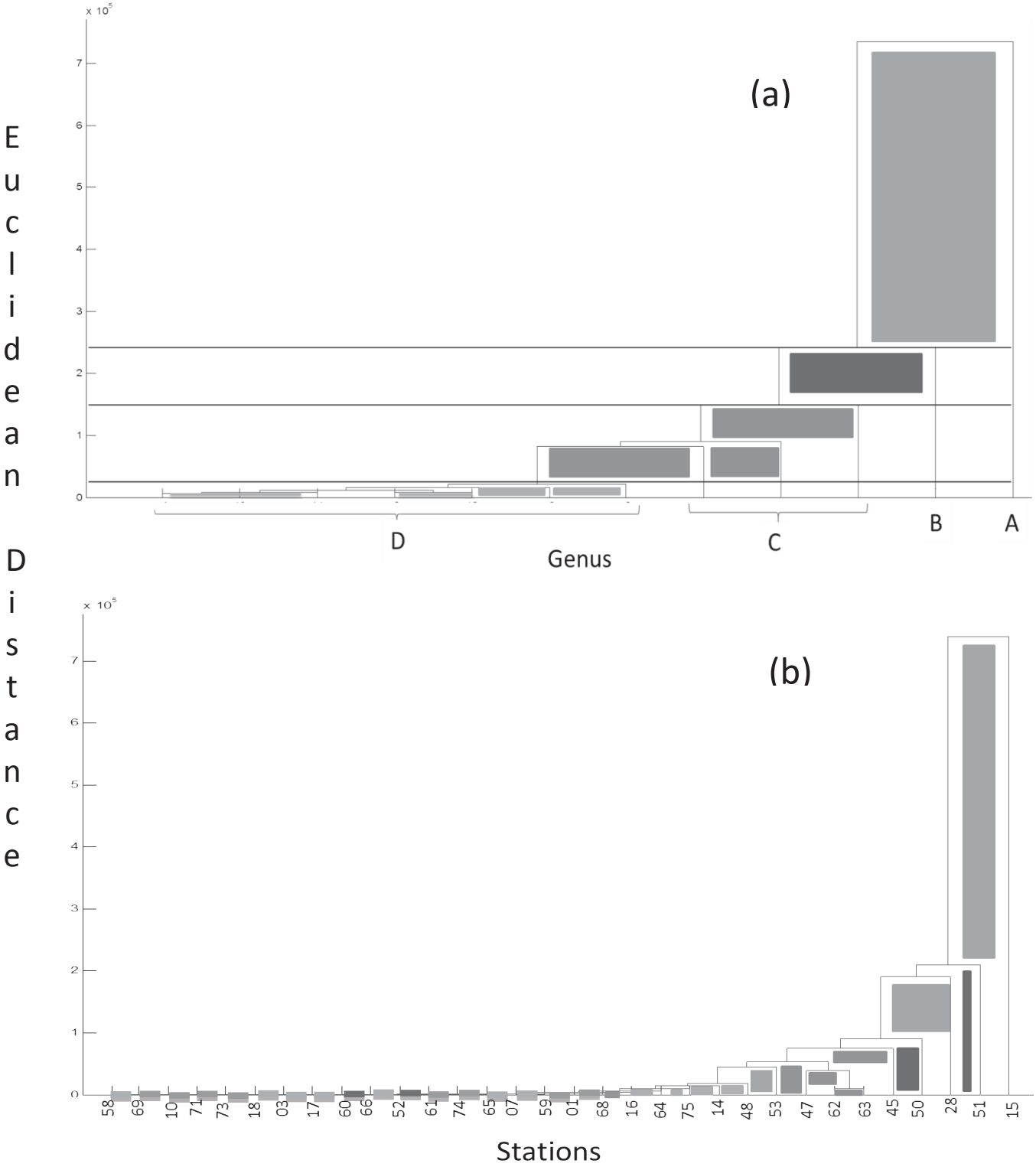

Figure 4. Hierarchical cluster dendrogram based in twelve dominants genus from Amplitude Niche Index and stations. The samples were taken at 10 metre depth during April 2008.

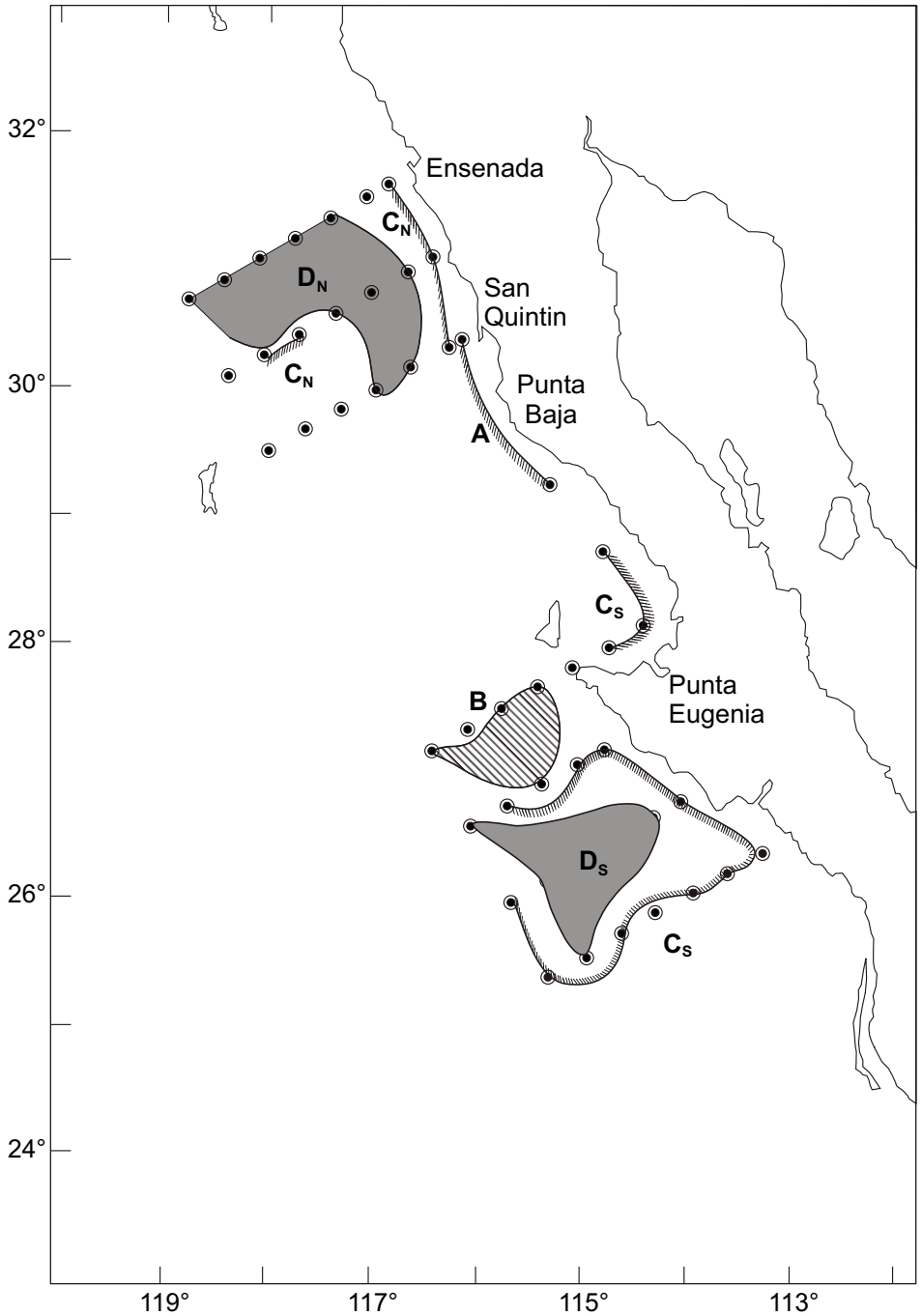

Figure 5. Phytogeographic provinces off Baja California: A (dominant *Eucampia* spp., bloom), B (weak *Pseudo-nitzschia* spp., bloom), C_{NORTH} and C_{SOUTH} (*Thalassiosira*, *Chaetoceros*, *Nitzschia*, *Fragilariopsis*, *Rhizosolenia*), and D_{NORTH} and D_{SOUTH} (*Thalassionema*, *Coscinodiscus*, *Guinardia*, *Actinoptychus*, *Navicula*). The samples were taken at 10 m depth during April 2008.

from the homogeneity of slopes between 440–550 nm (fig. 7). The PGPv A, PGPv B, and PGPv Cs show similar curves (fig. 6a, 6b, and 6d) with small differences in the shoulder between 440–550 nm (table 3), these three spectral shapes are related to upwelling events with the dominant group of diatoms (81%, 97%, and 99%). Conversely, to the PGPv CN, DN, and DS that showed a decrease of the diatom group (<71%), and less homogeneity of slopes and high diversity of nano-microphytoplankton (table 3).

DISCUSSION

The southern region of the California Current off Baja California presents productive oceanographic con-

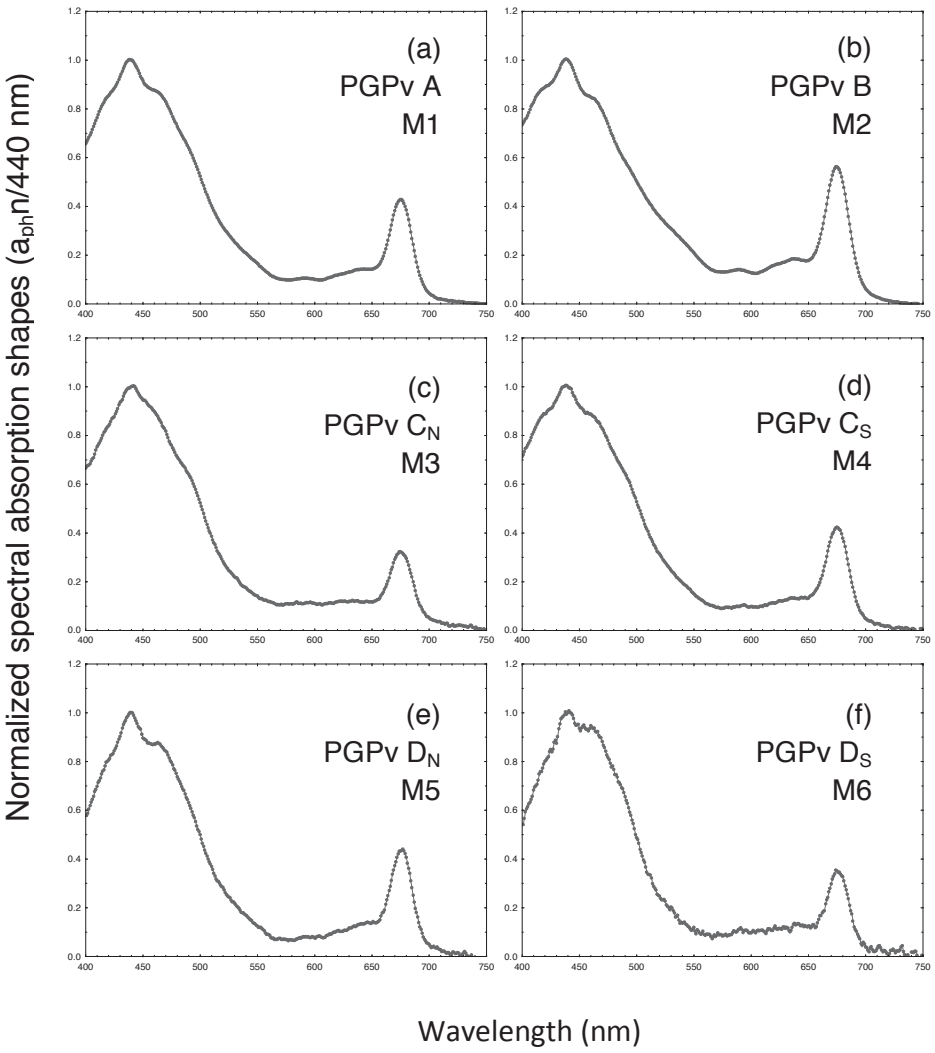

Figure 6. Normalized spectral absorption shapes (a_{ph}n/440 nm). The pattern curves represent the phytogeographic provinces: (a) M1 (PGPv A); (b) M2 (PGPv B); (c) M3 (PGPv C_{NORTH}); (d) M4 (PGPv C_{SOUTH}); (e) M5 (PGPv D_{NORTH}); (f) M6 (PGPv D_{SOUTH}). The spectral shapes are representative of 10 m depth during April 2008.

ditions, mainly in areas were upwelling events occur. In this study, two important upwelling events were detected in relation to the inclination of the mean $25\sigma_\theta$ surface. This inclination technique has been used off Baja California because the depth of mixing in the IMECOCAL area is found close to the pycnocline (Jerónimo-Moreno and Gómez-Valdéz 2006). The most intense upwelling event occurred off San Quintín Bay with the surficial part ($25\sigma_\theta$) near the coast, between stations 16 and 17, and the deepest part offshore, reaching ~80 m depth (fig. 8a). These data are similar to those reported off Baja California during the period 1998–2005 by Jerónimo-Moreno and Gómez-Valdéz 2006, where the deep inclination of $25\sigma_\theta$ reached 74 m. The second upwelling event showed oceanographic characteristics corresponding to weak upwelling conditions off Punta Eugenia, with the surficial part in the stations 47 and 50 and the deepest part offshore, reaching ~30 m depth (fig. 8c). Both these events produced phytoplankton blooms. The first event was dominated by *Eucampia* spp., with an abundance of 726×10^3 cells L^{-1} and an approximate biomass of 2657 μg C L^{-1}, whereas species of *Nitzschia* were observed in the weak event, with an abundance of 213×10^3 cells L^{-1} and a biomass of ~400 μg C L^{-1} (table 2, phytoplankton biomass not data show).

Based on temperature-salinity diagrams and chemical-biological data, authors such as Venrick et al. 2003, Baumgartner et al. 2008, Millán-Núñez and Millán-Núñez 2010, and Durazo et al. 2010 have detected that the SAW water mass off southern California shows high-nutrient, low-chlorophyll characteristics (NO_3 =10 μM, PO_4 =1 μM, Chl *a* =0.2 mg m^{-3}) and that it extends to 28°N, as observed in the present study, where salinity <33.5 reached transects 107 and 120 (fig. 8b, 8d). The

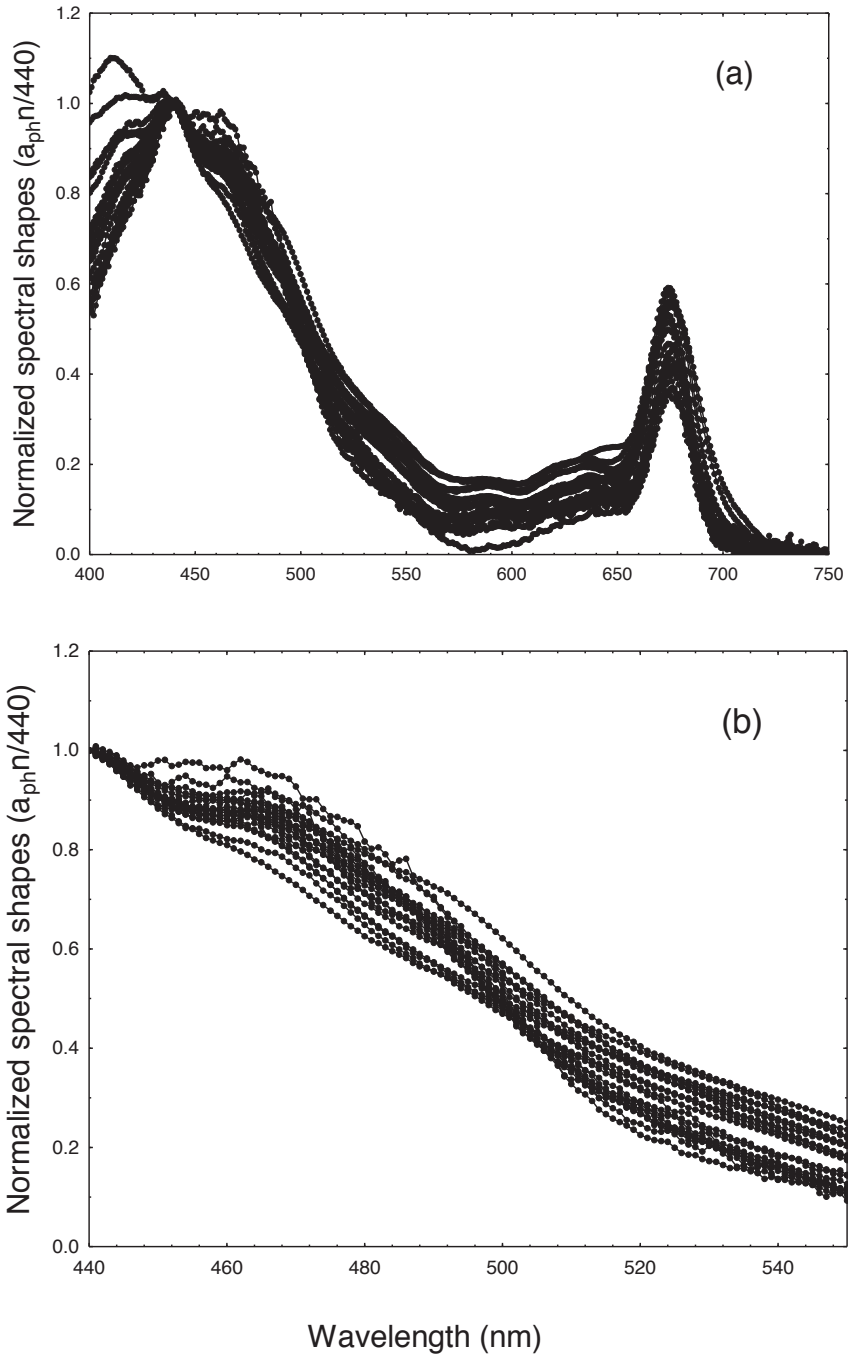

Figure 7. Normalized spectral shapes (a_{ph}n/440 nm) and homogeneity of slopes. a) All spectral shapes (400–750 nm), b) 440–550 nm.

geographic position of Punta Eugenia allows the observation of trajectory-effects of SAW off Baja California, hence, it should be possible to detect mixing processes of the hierarchical structure of the pelagic community, such as phytoplankton/zooplankton and fish eggs/larvae relationships. Here, we observed that SAW impacted the southern region of the California Current off Baja California (trans. 100, 103, 107), with an impoverished nanomicrodiatom structure at offshore stations, as opposed to coastal ones that were favored by local upwelling events. According to Tetsuichi et al. 2009, the Subarctic North Pacific is one of the major regions of the global ocean, with ~0.4 mg m^{-3} of Chl *a* concentration throughout the year; this value is similar to our offshore data of ~0.26 mg m^{-3} (table 2). All stations nearest to shore had very high chlorophyll (~7.84 mg m^{-3}), as shown in Fig-

TABLE 3
Phytogeographic provinces (PGPv) associated from stations, phytoplankton groups, and spectral absorption shapes. Pattern curves that conformed the spectral absorption shapes, dinoflagellates/diatoms rates (%), homogeneity of slopes (440–550 nm) from 10 m samples collected during April 2008.

Phytogeography Provinces (PGPv)	Spectral Shapes pattern curves	Stations	Taxonomic Groups (%) Diatoms/Dinoflag Mean Rates	Homogeneity Slopes (440–550 nm)
A	M1	15,28	97	–0.0081
B	M2	50,51,53	99	–0.0080
C_N	M3	1,9,10,14	53	–0.0074
C_S	M4	47,48,59,61,62,63,73,74	81	–0.0083
D_N	M5	4,6,17,18	47	–0.0091
D_S	M6	64,65,66,70	71	–0.0098

TABLE 4
Vertical distribution of nano-microdiatoms genera (>5 µm) at stations 6, 11, 18, 50. The numbers represent the natural logarithm of the cells L^{-1}. Data collected at 0, 10, 20, 50, 100 m depth during April 2008.

Stations	(		6		)	(		11		)	(		18		)	(		50		)
Depth	0	10	20	50	100	0	10	20	50	100	0	10	20	50	100	0	10	20	50	100
Diatoms																				
Nitzschia		5.62		6.30	4.92	6.87	6.02	4.92	5.62	4.92	4.92	4.92	4.92	7.00	7.48	7.69	9.56	8.44	7.69	6.68
Coscinodiscus	4.92	5.62						4.92	7.12			5.62		4.92	6.31	8.75	8.32	8.44	6.71	4.92
Pseudonitzschia								6.02						6.31		12.58	12.27	12.07	10.05	4.92
Ditylum															4.92	7.91	9.11	7.40	6.71	4.92
Thalassiosira																7.69	8.38	7.56	5.61	
Chaetoceros						4.92			4.92					6.31		9.97	9.40	8.01	6.71	
Rhizosolenia						6.53		7.00	5.62	4.92			4.92	5.62		9.08	9.87	10.19	8.87	
Eucampia																9.60	10.10	9.33		
Skeletonema																	8.10	7.40		
Thalassionema														6.02	5.62		5.61	6.71		
Stephanophyxis																	5.61			
Navicula		6.02			4.92	6.53	6.31	5.62	4.92			4.92	4.92	5.62			5.61			
Hemialus																	5.62			
Asterionella																	6.10			
Planktoniella									5.62											
Fragilariopsis									7.56	6.53										
Bacteriastrum								5.62												
Guinardia														6.02						

ure 3 where the Chl *a* is clearly related to distance from shore; the station that is numbered as #1 is the nearshore station, and #7 the offshore station. On the other hand, the vertical distribution of nano-microdiatoms at stations 6, 11, and 18 supports the idea of SAW input, with low phytoplankton abundance and low Chl *a* off Baja California (table 4).

In general, the spectral shapes of the PGPv showed similar pattern curves (fig. 6), with slight homogeneity slopes at the shoulder between 440–550 nm attributed to the different photosynthetic pigments of the associated organisms. A particular spectral shape was observed at station 15 and 28 (fig. 6a), with a slight difference in slope relative to Figure 6b stations 50, 51, and 53 (table 3). This was due to the dominance of *Eucampia* spp. (72%), and we thus consider that the spectral shape observed in Figure 6a is a reflection biomarker of the dominant pigment species; similar to the case of *Pseudo-nitzschia* spp., which had a predominance of 95% (fig. 6b).

The absorption Blue/Red ratios and Chl *a* concentrations in this cruise showed significant changes at 10 m of depth (table 2). In the offshore stations B/R ratios were greater than 3.5 with Chl *a* lower than 0.5 mg m^{-3} (fig. 3). This implies the predominance of picoplankton cells in the size structure of phytoplankton communities (Stramski and Morel 1990; Wu et al. 2007; Millán-Núñez and Millán-Núñez 2010; Goericke 2011). The inshore stations were different, with the B/R ratios (station 15, 28, 61, 62, 63, 64) dropping from 2.8 to 1.6, suggesting an increase in the proportion of nano-microdiatoms in the size structure of phytoplankton communities and Chl *a* concentration. We concluded that the southern region of the California Current off Baja California consists of a basic structure composed of smaller cells and scant microphytoplankton cells that maintains a balanced

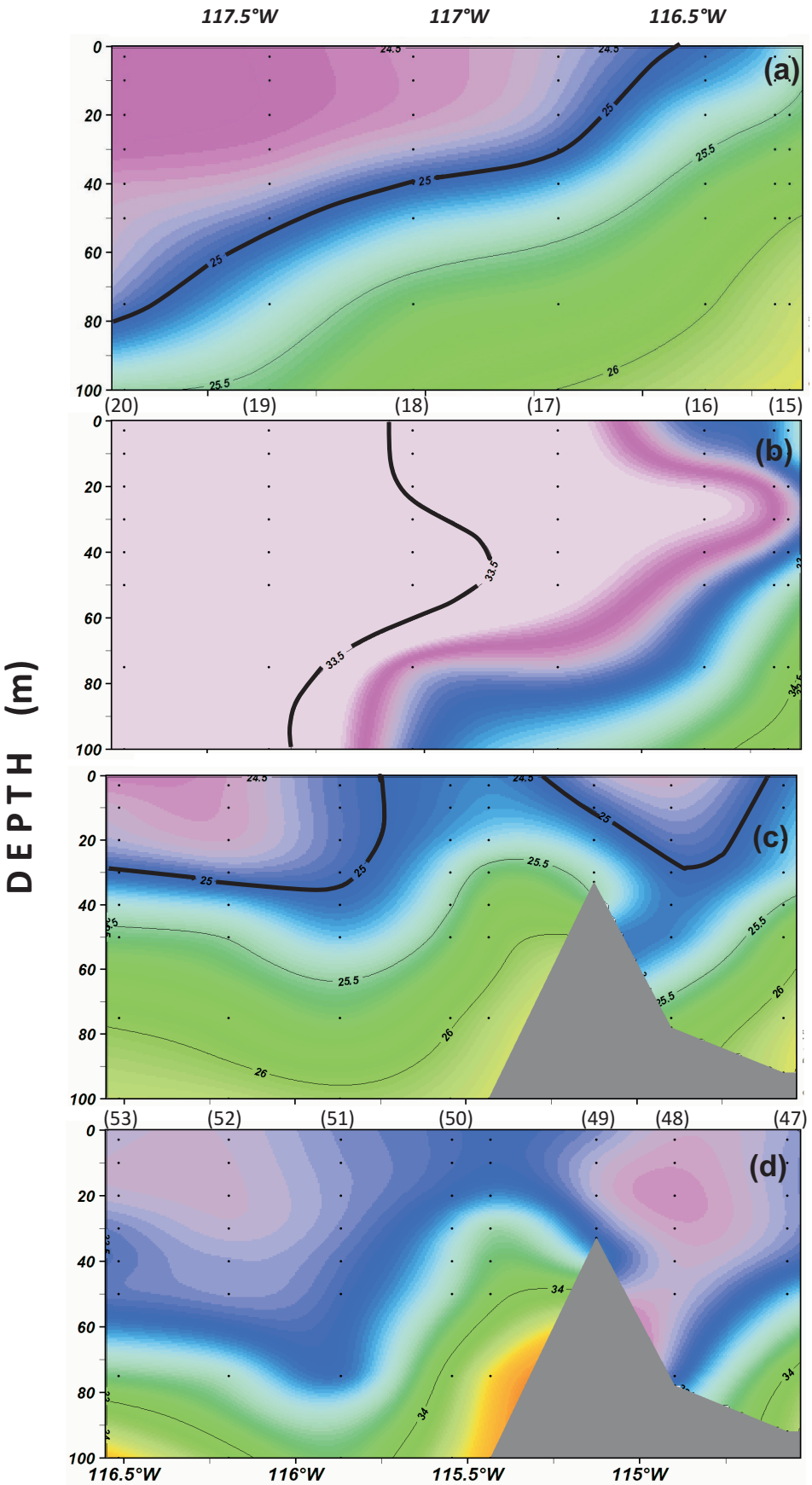

Figure 8. Vertical sections: (a) potential density (b) potential salinity along transect 107, and (c) potential density (d) potential salinity along transect 120. Numbers on top represent the station number along each transect.

community; periodically, an extra diatom population is superimposed on the basic structure, which results in high values of the absorption coefficient of phytoplankton and a better hierarchical phytoplankton structure in the upwelling system off Baja California.

ACKNOWLEDGEMENTS

I am grateful to the crew of the R/V *Francisco de Ulloa* for their efficient help on board: J. F. Moreno-Higareda, J. L. Cadena-Ramírez, M. E. De la Cruz-Orozco. We also want to thank J. M. Dominguez and F. J. Ponce for improving the drawings, and C. Harris for fine-tuning the English. The research was supported by a grant from IMECOCAL program and the Mexican Council for Science and Technology (CONACyT #23804 and #99252).

LITERATURE CITED

Baumgartner, T. R., R. Durazo, B. E. Lavaniegos, G. Gaxiola-Castro, J. Gomez-Valdéz, and J.García. 2008. Ten years of change from IMECOCAL observations in the southern region of the California Current Ecosystem. *GLOBEC* Inter., 14: 42–54.

Bjorkstedt, E. P., R. Goericke, S. McClatchie, E. Weber, W. Watson, N. Lo, B. Peterson, B. Emmett, J. Peterson, R. Durazo, G. Gaxiola-Castro, F. Chavez, J. T. Pennington, C. A. Collin, J. Field, S. Ralston, K. Sakuma, S. J. Bograd, F. B. Schwing, Y. Xue, W. J. Sydeman, S. Thompson, J. Santora, J. Largier, C. Halle, S. Morgan, S. K. Yong, K. P. B. Merkens, J. Hildebrand, and L. M. Munger. 2010. State of the California Current 2009–10: Regional variation persists through transition from La Niña to El Niño (and Back?). Cal. Coop. Oceanic Fish. Invest. Rep. 51: 1–31.

Cleveland, J. S., and A. D. Wiedemann. 1993. Quantifying absorption by aquatic particles: A multiple scattering correction for glass fiber filters. Limnol. Oceanogr., 38: 1321–1327.

Durazo, R. 2009. Climate and upper ocean varibility off Baja California, Mexico: 1997–2008. Progr. Oceanogr., 83: 361–368.

Durazo, R., A. M. Ramírez-Manguilar, L. E. Miranda, and L. A. Soto-Mardones. 2010. Climatología de variables hidrográficas. *In* Gaxiola-Castro G. and Durazo R. (ed.), dinámica del ecosistema pelágico frente a Baja California 1997–2007, pp. 21–57.

García-Córdova, J., R. Durazo, J. Gómez-Valdés, B. E. Lavaniegos, and G. Gaxiola-Castro. 2008. Informe de Datos de CTD. Campaña IMECOCAL 0804/05. B/O Francisco de Ulloa. Abril 16–mayo 1 de 2008. Techn. Rep. 79903. Biol. Ocanogr. Depart., CICESE., pp. 91.

Gaxiola-Castro, G., R. Durazo, B. E. Lavaniegos, M. E. De la Cruz-Orozco, E. Millán-Núñez, L. Soto-Mardones, and J. Cepeda-Morales. 2008. Respuesta del ecosistema pelágico a la variabilidad interanual del océano Pacífico frente a Baja California. Cienc. Mar., 34: 263–270.

Goericke, R. 2011. The size structure of marine phytoplankton—what are the rules? Calif. Coop. Oceanic Fish. Invest. Rep. 52: 198–204.

Jerónimo, G. and J. Gómez-Valdés. 2006. Promedios de temperatura y salinidad sobre una superficie isopícnica en la capa superior del océano frente a Baja California. Cienc. Mar., 32: 663–671.

Kishino, M., M. Takahashi, N. Okami, and S. Ichimura. 1985. Estimation of the spectral absorption coefficients of phytoplankton in the sea. Bull. of Mar. Sci., 37: 634–642.

Levins, R. 1978. Evolution in changing environments. Princ. Univ. Press. Princenton. 65 pp.

Macías-Carballo, M. 2011. Variabilidad de la forma espectral del fitoplancton y su relación taxonómica durante las primaveras del 2005–08 en la región occidental de Baja California. Master Sci. Thesis. CICESE, México., pp. 118.

Mantua, N. J., S. R. Hare, Y. Zhang, J. M. Wallace, and R. C. Francis. 1997. A Pacific decadal climate oscillation with impacts on salmon. Bull of the Amer. Meteor. Soc., 78: 1069–1079.

McClatchie, S., R. Goericke, F. Schwing, S. Bograd, W. Peterson, R. Emmett, R. Charter, W. Watson, N. Lo, K. Hill, C. Collins, M. Kahru, B. G. Mitchell, J. Koslow, J. Gómez-Valdés, B. E. Lavaniegos, G. Gaxiola-Castro, J. L. Gottschalck, M. Heureux, Y. Xue, M. Manzano-Sarabia, E. Bjorkstedt, S. Ralston, J. Field, L. Rogers-Bennet, L. Munger, G. Campbell, K. Merkens, D. Camacho, A. Harron, A. Douglas, and J. Hildebrand. 2009. The state of the California Current, spring 2008–09. Cold conditions drive regional differences in coastal production. Calif. Coop. Oceanic Fish. Invest. Rep. 50: 43–68.

Millán-Núñez, E., M. E. Sieracki, R. Millán-Núñez, J. R. Lara-Lara, G. Gaxiola-Castro, and C. C. Trees. 2004. Specific absorption coefficient and phytoplankton biomass in the southern region of the California Current. Deep-Sea Res II., 51: 817–826.

Millán-Núñez, E., and R. Millán-Núñez. 2010. Specific absorption coefficient and phytoplankton community structure in the southern region of the California Current during January 2002. J. Oceanogr., 66: 719–730.

Millán-Núñez, E. 2010. Variabilidad interanual del nano-microfitoplancton: inviernos 2001–07. *In*: Gaxiola-Castro, G., and R. Durazo (eds.). Dinamica del ecosistema pelágico frente a Baja California 1997–2007. SEMARNAT. Ensenada, Baja California. 241–262.

Mitchell, B. G. 1990. Algorithms for determining the absorption coefficient of aquatic particulates using the quantitative filter technique (QFT). SPIE Ocean Optic X, 1302: 135–148.

Moreno, J. L., S. Licea, and H. Santoyo. 1997. Diatomeas del Golfo de California, Univ. Auton. Baja California Sur., pp. 273.

Sokal, R. R. and F. J. Rohlf. 1962. The comparision of dendrograms by objective methods. Taxon., 11: 33–40.

Stramski, D. and A. Morel. 1990. Optical properties of photosynthetic picoplankton in different physiological states as affected by growth irradiance. Deep Sea Res., 37: 245–266.

Tetsuichi, F., K. Matsumoto, M. C. Honda, K. Hajime, and S. Watanabe. 2009. Phytoplankton composition in the subarctic North Pacific during autumn 2005. J. of Plank. Res., 31: 179–191.

Throndsen, J. 1978. Preservation and storage. In Sournia A. (ed.), Phytoplankton manual. UNESCO, Paris, pp. 69–74.

Tomas, C. S. 1997. Identifying marine phytoplankton. Academic Press, Inc. pp. 545.

Utermöhl, H. 1958. Vervolkommung der quantitativen phytoplankton methodik. Mitt. Int. Verein Theor. Angew. Limnol., 9, 1–38.

Venrick, E., S. J. Bograd, D. Checkley, R. Durazo, G. Gaxiola-Castro, J. Hunter, A. Huyer, K. D. Hyrenbach, B.E. Lavaniegos, A. Mantyla, F. B. Schwing, R. L. Smith, W. J. Sydeman, and P. A. Wheeler. 2003. The state of the California Current, 2002–03: Tropical and subarctic influences vie for dominance. Calif. Coop. Oceanic Fish. Invest. Rep. 44: 28–60.

Wolter, K. and M. S. Timlin. 1998. Measuring the strength of ENSO events—how does 1997/98 rank? Weather., 53: 315–324.

Wu, J., H. Hong, S. Shang, M. Dai, and Z. Lee. 2007. Variations of phytoplankton absorption coefficients in the northern South China Sea during spring and autumn. Biogeosci. Dissc., 4: 1555–1584.